

Correction of Terrestrial LiDAR Data Using a Hybrid Model

Wallace MUKUPA, China, Gethin Wyn ROBERTS, United Kingdom, Craig Matthew HANCOCK, China, Khalil AL-MANASIR, China.

Key words: Terrestrial Laser Scanning, LiDAR, Intensity Correction, Concrete

SUMMARY

The utilization of Terrestrial Laser Scanning (TLS) intensity data in the field of surveying engineering and many other disciplines is on the increase due to its wide applicability in studies such as change detection, deformation monitoring and material classification. Radiometric correction of TLS data is an important step in data processing so as to reduce the error in the data. In this paper, a hybrid method for correcting intensity data has been presented. The proposed hybrid method aims at addressing two issues. Firstly, the issue of near distance effects for scanning measurements that are taken at short distances (1 to 6 metres) and secondly, it takes into account the issue of target surface roughness as expounded in the Oren-Nayar reflectance model. The proposed hybrid method has been applied to correct concrete intensity data that was acquired using the Leica HDS7000 laser scanner. The results of this proposed correction model are presented to demonstrate its feasibility and validity.

1. INTRODUCTION

Correction of intensity data is essential due to systematic effects in the LiDAR system parameters and measurements and in order to ensure the best accuracy of the delivered products (Habib *et al.*, 2011). The whole aim of radiometric correction is to convert the laser returned intensity recorded by the laser scanner to a value that is proportional to the object reflectance (Antilla *et al.*, 2011). This correction of intensity data is still an open area of investigation and this is the case because even though a couple of researchers have studied the subject of TLS intensity correction for instance, a standard correction method that can be applicable for all the various types of laser scanners is non-existent (Penasa *et al.*, 2014). Such a scenario is also explained by some of the laser scanning research work that are still being published without the intensity data having been corrected (Krooks *et al.*, 2013). However, in Tan and Cheng (2015), it is purported that the proposed intensity correction method is suitable for all TLS instruments. In the case of Airborne Laser Scanning (ALS), the subject of intensity data correction has an old history compared to TLS and this has been reported by researchers such as Kaasalainen *et al.* (2011).

It has been reported that the effect of the measurement range (distance) on the intensity data depends on several parameters. In the case of TLS, the effects of the range tend to depend on the instrument especially when measurements are taken at close range to the target. The effects of the

range on TLS intensity or the dependence of the received power as a function of the range is proportional to $1/R^2$ (R = range) in the case of extended diffuse targets (Jelalian, 1992). This implies that the whole laser footprint is reflected on one surface and it has Lambertian scattering properties. However, non-extended diffuse targets exhibit different range dependencies. For instance, point targets (e.g. a leaf) with an area smaller than the footprint are range independent and targets with linear physical properties (e.g. wire) are linear range dependent. Therefore, the range dependency becomes $1/R^4$ for targets smaller than laser footprint size and $1/R^3$ for linear targets (Vain and Kaasalainen, 2011).

According to Krooks *et al.* (2013), different scanners have different instrumental effects on the measured intensity and this implies that it is prudent to study each scanner individually. Instrumental effects have been reported to affect the intensity recorded for TLS instruments. Even though distance has been predicted to follow the range squared inverse ($1/R^2$) dependency for extended targets based on the physical model (radar equation), in practical applications this prediction is inapplicable at all ranges because of TLS instrumental modifications that are designed to enhance the range measurement determination (Holfe and Pfeifer, 2007; Balduzzi *et al.*, 2011; Antilla *et al.*, 2011). In a similar vein, Kaasalainen *et al.* (2011) state that the knowledge of the TLS instrument as to whether it has near-distance reducers or logarithmic amplifiers in the case of small reflectance is of cardinal importance in an attempt to know the distance effects and the extent to which the measured intensity is affected by instrumental effects. In Kaasalainen *et al.* (2009a) it has been reported that measurement of the intensity taken at short ranges, 1m in this case have been significantly affected at such near distances by brightness reducers.

The effects of the incidence angle on the intensity are related to the scanned target object in terms of its surface structure and scattering properties (Krooks *et al.*, 2013). In terms of the rugosity of the target, macroscopic irregularities of the order of mm to cm size and almost the same size as the laser footprint, neutralize the effects of the incidence angle on the intensity. This is so because there are always elements on the surface of the target that are perpendicular to the incident laser beam (Kaasalainen *et al.*, 2011). In a similar vein Penasa *et al.* (2014) states that the effects of the scattering angle can be neglected if the surface roughness of the target is comparable with the laser spot size. Other studies for instance Kaasalainen *et al.* (2009b) showed that the significance of the angle of incidence only becomes an important parameters when it is greater than 20° for several materials. The strength of the signal that the scanner receives is dependent on the backscattering properties of the target scanned (Shan and Toth, 2009). If the surface backscattering the laser is an extended target and a Lambertian reflector, the backscatter strength in the angular domain depends entirely on the incidence angle.

Different TLS intensity correction models have been proposed and some methods are based on the physical model (laser range equation) whereas others are modified versions of the physical model and some are data driven. For instance in Balduzzi *et al.* (2011) the modified radar range equation was used to correct the intensity data. It is reported that the laser scanner (FARO LS880) which was used has an intensity filter and with the assumption that this filter has only an impact on the

intensity variations due to distance, the range squared inverse law was replaced by a device specific distance function and then a logarithmic function was applied. In Kaasalainen *et al.* (2008), an important consideration was the effect of the logarithmic amplifier of the FARO LS HE80 for small reflectance. The logarithmic correction was calibrated by fitting an exponential function.

In Penasa *et al.* (2014) an intensity correction approach for distance effects and exclusive of other variables such as incidence angle or atmospheric losses is presented. The correction approach did not apply the radar equation instead it is stated that the correction was based on estimating a correcting intensity-distance function on an appropriate reference point cloud via a Nadaraya–Watson regression estimator. In Blaskow and Schneider (2014) an intensity correction approach is presented which involves polynomial approximation and static correction model. Under the polynomial approximation, the intensity-distance curves were functionalised as basis for the static correction model and the Spectralon target data served as reference. Pfeifer *et al.* (2007) investigated data driven models and a function, $F(\rho, \alpha, r)$ was sought to predict the intensity value from range (r), reflectivity (ρ) and incidence angle (α). To correct the intensity for the effects of target reflectivity and incidence angle, different functions were tested. The function which brought the curves to the closest overlap was $(\rho \cos(\alpha))^{-0.16}$ and all intensity values were then multiplied by this function to remove the influence of target reflectivity and angle of incidence. Two linear functions were then fitted to correct the intensity for distance effects. In Franceschi *et al.* (2009) a study was undertaken that focused on using TLS intensity data to discriminate between marls and limestone, the corrected intensity was taken to be related and proportional to the target reflectivity and an assumption was made that the scanned objects were Lambertian reflectors.

In Fang *et al.* (2015) an intensity correction method is presented based on estimating the laser transmission function so as to determine the ratio of the input laser signal between the limited and the unlimited ranges and then integrating this ratio in the radar range equation in order to correct the intensity data near distance effects. Tan and Cheng (2015) developed a model to correct the effects of the angle of incidence and the distance on the intensity data. The proposed correction model is approximated by a polynomial series based on the Weierstrass approximation theory and an approach to estimating the specific parameters is presented. Using a similar approach, Tan *et al.* (2016) proposed an intensity correction method for distance effects where the range squared inverse law as described in the radar equation and the ALS range correction methods was replaced by a polynomial function of distance. Zhu *et al.* (2015) investigated the use of TLS intensity data to detect leaf water content and an intensity correction method is described where firstly a reflection model was employed to get rid of specular reflection which was as a result of leaf surface at perpendicular angle and then reference targets were utilised to correct the effects of the angle of incidence.

In view of the above, this study aimed at correcting the TLS returned intensity for concrete by looking at methods of modelling the variables that have an effect on the intensity values of the laser in this case the effects of the measurement range and incident angle since the experiment was carried out in a controlled environment. The focus of the investigation was to use existing models of

laser behaviour to develop a correction model for TLS intensity data that is also capable of addressing near-distance effects and surface roughness of the target since not all objects are perfect Lambertian reflectors. The proposed hybrid intensity correction method is based on the radar equation (Jelalian, 1992), near-distance correction model (Fang *et al.*, 2015) and the Oren-Nayar reflectance model (Carrea *et al.*, 2016). These existing models and the development of a hybrid intensity correction model are explained in detail in the data processing section. A description of the experimental procedure for testing the proposed hybrid method for correcting intensity data is provided and the results of this correction model are presented to demonstrate the feasibility and validity of the method.

2. EXPERIMENTAL PROCEDURE

2.1 Target Objects: Concrete Specimens

Prismatic concrete beams (Fig. 1) were used as scanning target objects mainly because this is part of an on-going project investigating the use of laser intensity for the assessment of fire-damaged concrete. Since surface roughness of the scanned object was of interest in this study, it is worth mentioning that the concrete consisted of fine aggregate (river sand) with a maximum grain size of 5 mm and crushed siliceous coarse aggregate with a diameter ranging from 5 to 20 mm. For easy identification, the concrete specimens were labelled as: Block C, Block 1, Block 2, Block 3 and Block 4.



Fig. 1: Concrete specimens

2.2 Scanning Room and Equipment

The experiments were conducted under controlled laboratory conditions. The factors affecting the returned intensity under such conditions are the scanning geometry and the instrumental effects. Since the experiments were carried out in a controlled environment and at short range (1 to 6m), atmospheric losses were neglected. The Leica HDS7000 laser scanner (Fig. 2) was used to scan the

concrete specimens and the technical specifications of this scanner are as presented in Table 1 below.



Fig 2: HDS7000 Laser Scanner

Table 1: Specification of TLS Instrument

<i>Scanner</i>	<i>Leica HDS7000</i>
Ranging method	Phase
Wavelength	1500nm
Field of View (Ver/Hor)	320° x 360°
Laser Class	1
Range	0.3-187m
Linearity error	≤1mm
Samples/sec	1016000
Beam diameter	~3.5mm @ 0.1m
Beam divergence	< 0.3 mrad
Temp Range	0-45°C
Colour	External
Weight	9.8kg

Source: Leica Geosystems (2012)

2.3 Measurement Setup and Data Acquisition

The measurement distances between the HDS7000 scanner and the target objects (concrete specimens) were ranging from 1 to 6 metres and the total station was utilized in marking out the scanning distances. The steel frame where the blocks were placed was levelled using a spirit level and then the distance to the prism placed right on the edge and centre of the steel frame was measured. Distances up to 6m in steps of 1m were measured using a total station so as to have scans taken from well-known accurate distances. The geometry of the experiment in terms of scanning measurement setup is shown in Fig. 3.

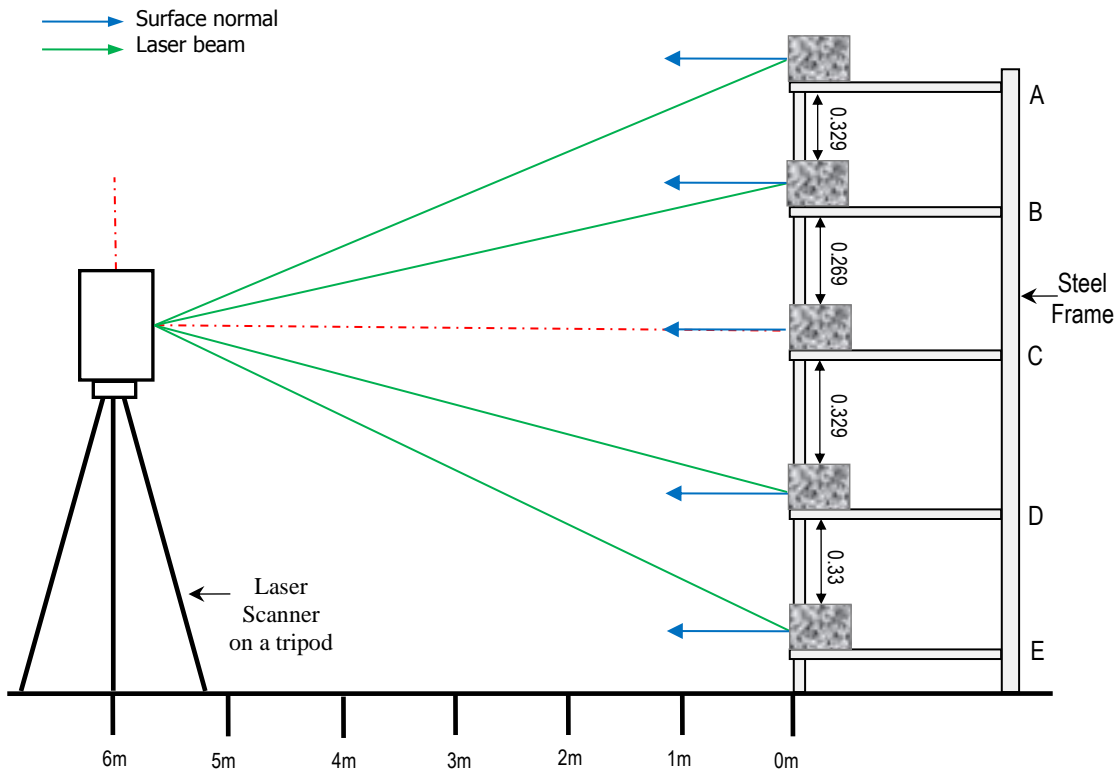


Fig. 3: Laser scanner and blocks at different levels on a frame (Letters A, B, C, D and E stand for shelf levels).

With reference to Fig. 3, the planar surface of each concrete block was properly aligned with the frame edge with the aid of a mark which was made on the centre of the block and the frame too. These measures were carried out so as to position each concrete block at approximately the same required distance from the scanner for each respective scanning session. Independent measurements using a steel rule and tape were carried out to ensure that each concrete block was accurately oriented. The experiment was set-up this way in order to only focus on the scanning geometry which consists of the angle of incidence and the range between the scanner and the target object (Krooks *et al.*, 2013; Kaasalainen *et al.*, 2011) as the factor influencing the poor laser returned signal. The concrete blocks were placed at different heights on shelves of the steel frame with the control block on the centre shelf at the same height as the scanner with its front face approximately vertical and perpendicular to ensure that scanning was done at roughly normal angle of incidence. The scanning parameters used in the experiments involved super high resolution and a normal quality.

3. DATA PROCESSING

3.1 Scan Data Pre-processing

The HDS7000 scans were converted to text files (.pts format) using the Z + F laser control software instead of the Leica Cyclone software as it has been reported for instance in Kaasalainen *et al.* (2011) that this software scales the intensity so as to accentuate visualisation. The scans which were converted to text files contained the geometric data in terms of X, Y and Z coordinates in a Cartesian coordinate system as well as radiometric data i.e. the intensity values for the 3D coordinates. The intensity values of data converted to text files were ranging from -2047 to +2048. The output Cartesian coordinates can be converted to spherical (range, zenith and azimuth angles) coordinates based on a zero origin for the TLS instrument as described in Eq. (1) (Soudarissanane *et al.*, 2009):

$$\begin{bmatrix} R_i \\ \theta_i \\ \phi_i \end{bmatrix}_{i=1\dots n} = \begin{bmatrix} \sqrt{x_i^2 + y_i^2 + z_i^2} \\ \tan^{-1} \left(\frac{y_i}{x_i} \right) \\ \tan^{-1} \left(\frac{z_i}{\sqrt{x_i^2 + y_i^2}} \right) \end{bmatrix}_{i=1\dots n} \quad [1]$$

3.2 Intensity Data Correction

The proposed hybrid intensity correction method consists of two parts, namely the near-distance correction model in Fang *et al.* (2015) and the Oren-Nayar correction model described in Carrea *et al.* (2016). In principle, the hybrid intensity correction method has a basis in the radar (range) equation (Eq. (2)) and so an overview of this equation is presented and then it is followed by the correction for near-distance effects and the Oren-Nayar reflection model. The radar (range) equation (Eq. (2)) consists of three main components and these are: the sensor, the target and the environmental parameters which diminish the amount of power transmitted. Importantly, this equation (Eq. (2)) has been applied as a physical model for the correction of laser intensity data (Yan and Shaker, 2014) in several studies where the equation has been applied either as it is or in a modified form.

$$P_r = \frac{P_t D_r^2}{4\pi R^4 \beta_t^2} \eta_{sys} \eta_{atm} \sigma \quad [2]$$

Where P_r is the received power, P_t is the power transmitted, D_r is the receiver aperture, R is the range between the scanner and the target, β_t is the laser beam width, σ is the cross-section of the target, η_{sys} and η_{atm} are system and atmospheric factors respectively. The cross-section σ can be described as follows (Höfle and Pfeifer, 2007):

$$\sigma = \frac{4\pi}{\Omega}\rho A_s \quad [3]$$

Where Ω is the scattering solid angle of the target, ρ is the reflectivity of the target and A_s the area illumination by the laser beam. Under the following assumptions Eq. (3) can be simplified. First, the entire footprint is reflected on one surface and the target area illumination A_s is circular, hence defined by the range R and laser beam width β . Secondly, the target has a solid angle of π steradian ($\Omega = 2\pi$ for scattering into half sphere). Thirdly, the surface has Lambertian scattering characteristics. If the incidence angles are greater than zero ($\alpha > 0^\circ$), σ has a proportionality of $\cos \alpha$ (Höfle and Pfeifer, 2007):

$$A_s = \frac{\pi R^2 \beta_t^2}{4} \quad [4]$$

Substituting A_s in Eq. (4) into Eq. (3) leads to:

$$\sigma = \pi \rho R^2 \beta_t^2 \cos \alpha \quad [5]$$

Substituting Eq. (5) into Eq. (2) results into a squared range which is inversely related to the returned laser signal (Eq. (6)), and independent of the laser beam width (Höfle and Pfeifer, 2007).

$$P_r = \frac{P_t D_r^2 \rho}{4R^2} \eta_{sys} \eta_{atm} \cos \alpha \quad [6]$$

Considering the assumption that the target object has Lambertian scattering properties and covers the entire hemisphere implies a solid angle of π steradian and so the effective aperture $D_r^2 = 4$ is equivalent to π . With these assumptions factored into Eq. (2), the radar range equation can be rewritten as described in Eq. (7) (Soudarissanane *et al.*, 2011):

$$P_r = \frac{P_t \cos \alpha}{R^2} \pi \rho \eta_{sys} \eta_{atm} \quad [7]$$

In terms of TLS systems, Eq. (7) can be written as:

$$P_r = \frac{K \rho \cos \alpha}{R^2} \quad [8]$$

Where the term $K = (P_t D_r^2 / 4) \eta_{sys} \eta_{atm}$ in the original radar range equation (Eq. (2)) is taken to be a constant. The power received, P_r is taken to be equivalent to the recorded laser returned intensity. The reflectance, incidence angle and range parameters are as defined above. Eq. (8) is not an ideal physical model for all scenarios and this is so because for most scanners, the intensity-distance correction tends to be affected more by instrumental effects and these occur either for

measurements taken at shorter baselines or those taken at longer baselines (Balduzzi *et al.*, 2011).

3.2.1 Near-Distance Correction Model

A number of researchers (e.g. Krooks *et al.*, 2013) have reported that the effects of the scanning distance and the incidence angle on the intensity do not mix, implying that it is possible to solve these effects independent of each other. According to Fang *et al.* (2015), solving for the near-distance effects on the intensity involved considering several parameters such as the Gaussian laser beam, the lens formula, focusing of the lens and the computation of the detector's received power under the assumption that it is circular. In order to avoid repetition, detailed information can be found in Fang *et al.* (2015) and where it has been stated that for a coaxial laser scanner, the near-distance effect can be described as the ratio of the input laser signal that the detector captures between the limited range (R) and unlimited range (∞) as shown in Eq. (9):

$$\eta(R) = \frac{P(R)}{p(\infty)} = 1 - \exp\left\{\frac{-2r_d^2(R+d)^2}{D^2\left[\left(1-\frac{s_d}{f}\right)R+d-\frac{ds_d}{f}+s_d\right]^2}\right\} \quad [9]$$

Where r_d is the radius of the circular laser detector, d is the offset between the measured range R and the object distance from the lens plane, D is the diameter of the lens, S_d is the fixed distance of the detector from the lens and f is the focal length. All of which are parameters of the laser scanner. Combining Eq. (9) with Eq. (8) and taking into account the near-distance effect, the recorded raw intensity (I_{raw}) value can be written as:

$$I_{raw} \propto P_r = \eta(R) \frac{K\rho\cos\alpha}{R^2} \quad [10]$$

3.2.2 Oren–Nayar Reflectance Model vis-à-vis Target Surface Roughness

An investigation which considered faceted surfaces in an attempt to describe surface roughness was addressed in the Oren-Nayar reflectance model (Oren and Nayar, 1994; Oren and Nayar, 1995) which makes a prediction that a surface with facets returns more light in the direction of the light source than a surface with Lambertian properties. For a faceted surface, other than the global normal, each micro-facet has its own normal and orientation. For some surfaces, each facet can actually be a perfect diffuse reflector though this may not be so when all the various facets are combined (Carrea *et al.*, 2016). However, in a case where the various facets are of the same size or smaller than the wavelength, the behaviour tends to follow that of diffuse reflection. But in a case where the facets are of a size that is almost as large as the laser beam spot size, the returned intensity gets controlled by a few facets.

In the Oren-Nayar reflectance model, an important parameter which models the effect of a faceted surface on reflection is presented. This parameter is the standard deviation of the slope angle of facets (σ_{slope}) and it can be computed for different reflectivity surfaces. The Oren–Nayar model is a Bidirectional Reflectance Distribution Function (BRDF) since it models the reflectance with regards to both the incidence and the reflection direction. The Oren–Nayar model is expressed in the following form where the radiance is computed as follows (Oren and Nayar, 1995):

$$L = \rho E_0 \cos \theta_i (A + B \text{Max}[0, \cos(\phi_r - \phi_i)] \sin \alpha \tan \omega) \quad [11.1]$$

$$A = 1.0 - 0.5 \frac{\sigma_{slope}^2}{\sigma_{slope}^2 + 0.33} \quad [11.2]$$

$$B = 0.45 \frac{\sigma_{slope}^2}{\sigma_{slope}^2 + 0.09} \quad [11.3]$$

Where L is the radiance, E_0 is the radiant flux received at normal incidence angle in radians, ρ is the material reflectivity, α is the incoming and ω the outgoing incidence angle, ϕ_r and ϕ_i are the reflected and incident viewing azimuth angle in radians and σ_{slope} as the standard deviation of the slope angle distribution in radians.

According to Carrea *et al.* (2016), the model Eq. (11) can be applied in TLS systems where in terms of the configuration, the incidence and reflected rays are coincident as expressed below:

$$\phi_r - \phi_i = 0 \xrightarrow{\text{yields}} \cos(\phi_r - \phi_i) = 1 \quad [12]$$

Therefore Eq. (11) which is a BRDF can be turned into a non-BRDF where α the incoming incidence angle is equal to ω the outgoing incidence angle and then rewritten as:

$$L = \rho E_0 \cos \alpha (A + B \sin \alpha \tan \alpha) \quad [13.1]$$

$$A = 1.0 - 0.5 \frac{\sigma_{slope}^2}{\sigma_{slope}^2 + 0.33} \quad [13.2]$$

$$B = 0.45 \frac{\sigma_{slope}^2}{\sigma_{slope}^2 + 0.09} \quad [13.3]$$

3.2.3 Hybrid Intensity Correction Model

Since Eq. (10) has K as a constant, it can be simplified and rewritten as:

$$I_{raw} = \eta(R) \frac{\rho \cos \alpha}{R^2} \quad [14]$$

The corrected intensity (I_{corr}) value can be computed as follows considering the near distance effects, material reflectivity, incidence angle and range:

$$I_{corr} = I_{raw} \cdot \left\{ \eta(R) \frac{\rho \cos \alpha}{R^2} \right\} \quad [15]$$

This intensity correction (Eq. (15)) can be used for perfect diffuse scattering surfaces. However, for surfaces with micro-facets this correction would not work well and so there is need to integrate the standard deviation of the slope angle since each facet on the surface has its own normal. Thus a hybrid intensity correction model that considers near distance effects and also integrates the Oren-Nayar model is proposed to improve the intensity correction.

$$I_{corr} = I_{raw} \cdot \left\{ \eta(R) \frac{\rho \cos \alpha (A + B \sin \alpha \tan \alpha)}{R^2} \right\} \quad [16.1]$$

$$A = 1.0 - 0.5 \frac{\sigma_{slope}^2}{\sigma_{slope}^2 + 0.33} \quad [16.2]$$

$$B = 0.45 \frac{\sigma_{slope}^2}{\sigma_{slope}^2 + 0.09} \quad [16.3]$$

The standard deviation of the slope angle of facets (σ_{slope}) was determined as in Carrea *et al.* (2016) and the following is an explanation of the procedure. To obtain the optimal value for the slope standard deviation (σ_{slope}), standardisation with respect to values close to normal incidence was computed by using a sub-sample of points that covered the area of the concrete block so as to reduce computational intensity. Since the concrete blocks were fairly rough and several points were scanned on the face on the block, it implies that each point had its own incidence angle dependent on where the laser hit on the block and the orientation of the normal at that position. This being the case, an optimisation function was employed in order to calculate the optimal value of σ_{slope} . Therefore, after the intensity was corrected for near distance effects, it was then vital to compute the optimal σ_{slope} value which would give a minimal variation of the corrected intensity by taking into consideration the different incidence angles. The optimisation function minimises the differences between the mean corrected intensity values for the two intervals of the incidence angle i.e. 0° to 10° and 0° to 45° by way of minimising to a single variable on a fixed interval and so making it possible to obtain the minimum of $f(\sigma_{slope})$ on a bounded interval $[0, 1]$ as written in Eq. (17) below:

$$\min_{0 \leq \sigma \leq 1} f(\sigma_{slope}) = \left| \frac{1}{n} \sum_{i=1}^n \left(I_{corr_{10^\circ}}(\sigma_{slope}) \right) - \frac{1}{n} \sum_{i=1}^n \left(I_{corr_{45^\circ}}(\sigma_{slope}) \right) \right| \quad [17]$$

The data processing and intensity correction method was implemented in Matlab routines. The intensity value is dimensionless and for each block, statistics such as intensity mean and standard deviation were calculated. The average roughness (σ_{slope}) values for the blocks were not so far away from 0° as values ranged from 1.15° to 2.58° . Concrete reflectivity measurements were not taken due to non-availability of the spectrometer which would measure reflectivity at a wavelength of 1500 nm (which is the wavelength of the HDS7000 laser scanner used in this study). However, we searched for documentation with concrete reflectivity information at the desired wavelength and information was found in Larsson *et al.* (2010). Based on this finding, the reflectance of concrete is in the range between 0.300 to 0.400 (Fig. 4) and since the concrete which was used in the study was gray and with some roughness, it was a trial and error of reflectance values from 0.370 to 0.400.

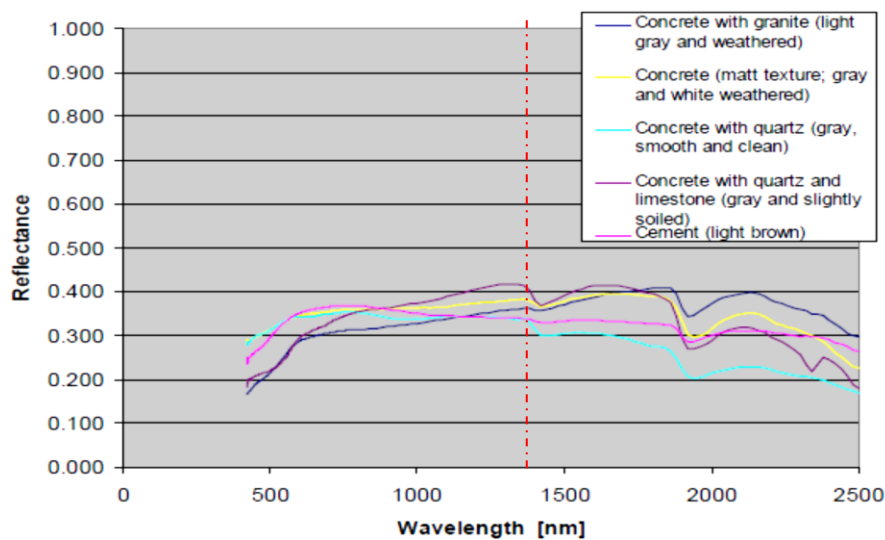


Fig. 4: Reflectivity spectrum of concrete and cement (Larsson *et al.*, 2010)

4. RESULTS AND ANALYSIS

4.1 Intensity Standard Deviation and Distribution of Data

The data acquired was analyzed to study for each block the relation between intensity standard deviation and intensity mean as was scanned at the five various incidence angles labelled A to E (see measurement setup in Fig. 3) and results are as shown in Fig. 5 below.

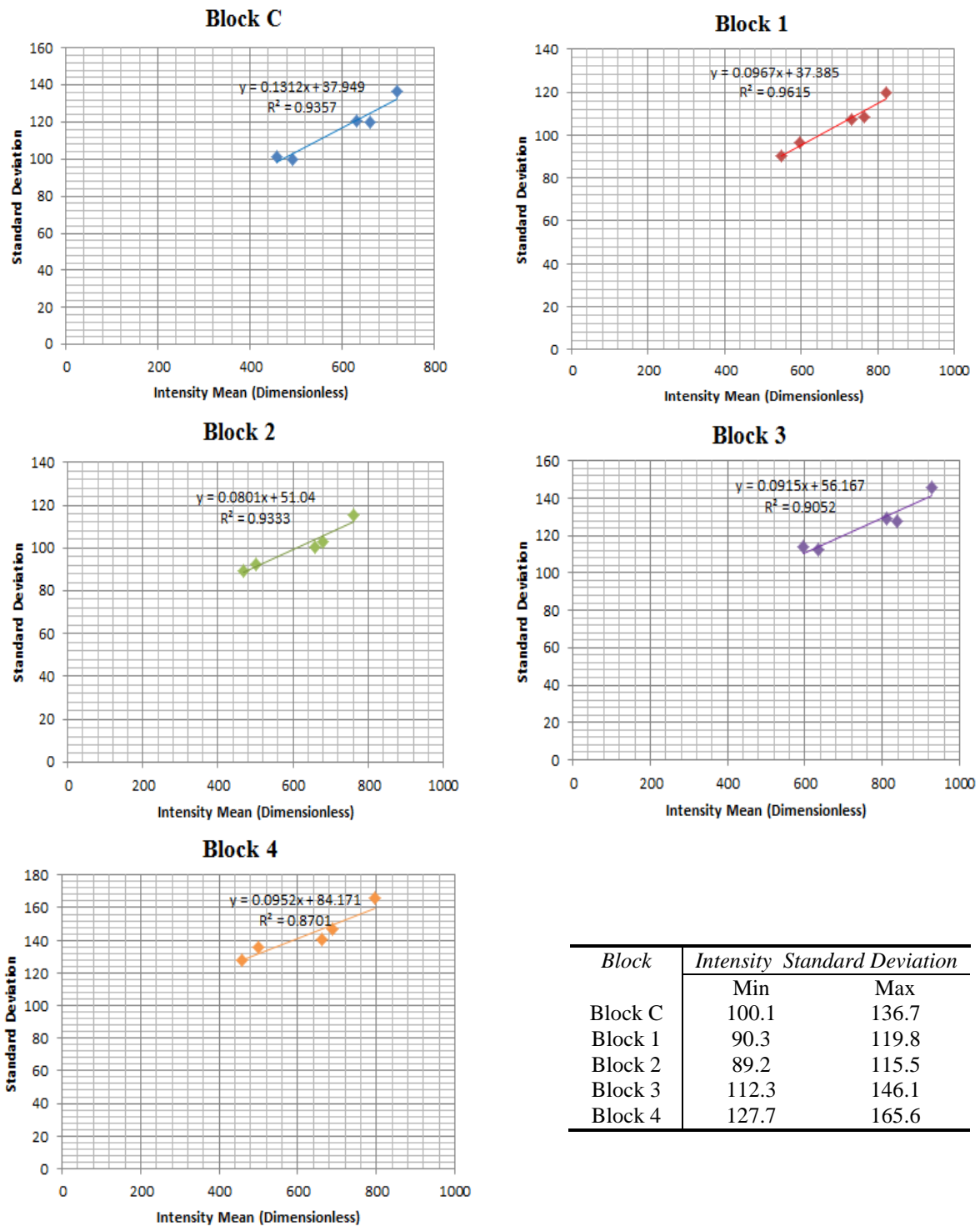
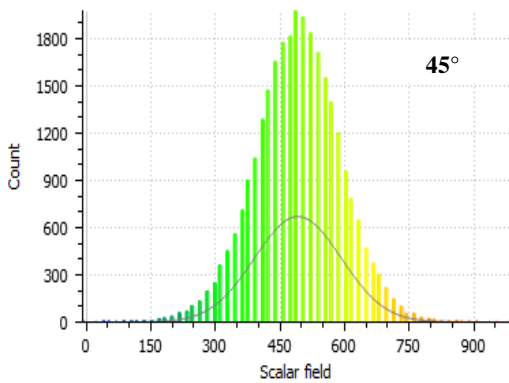


Fig. 5: Intensity standard deviation against intensity.

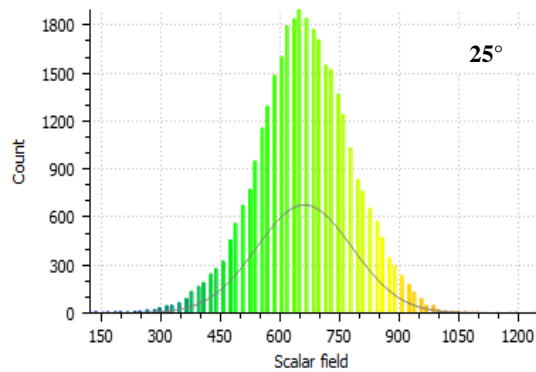
Apparently, the standard deviation grows with the intensity mean for each block and this is verified in Fig. 5. Regardless of the scanning incidence angles which were 45° , 25° , 0° , -25° and -45° , the strength of the linear relationship between the two variables in Fig. 5 is strong as can be seen by the values of the coefficient of determination for each block. The minimal variation of the coefficient of determination of the blocks is due to the fact that their surfaces were not totally homogenous because the concrete aggregate cannot be uniformly distributed in all blocks although the same mix design was used.

The distribution of the intensity data for the blocks scanned at various incidence angles was as assessed and taking Block C as an example, the results are as shown in Fig. 6.

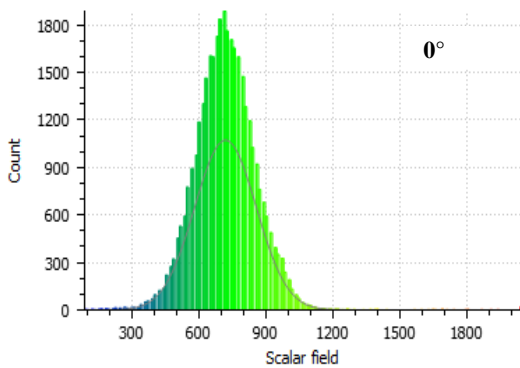
Gauss: mean = 491.797455 / std.dev. = 100.097382 [170 classes]



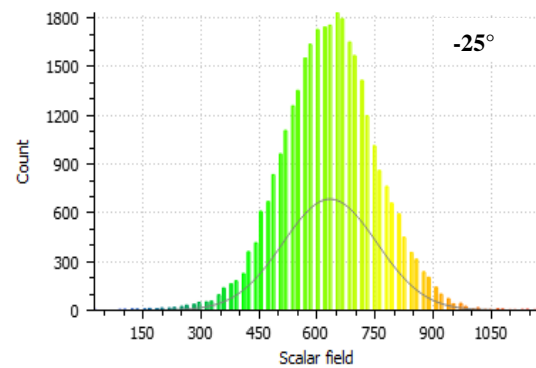
Gauss: mean = 661.177551 / std.dev. = 119.680962 [182 classes]



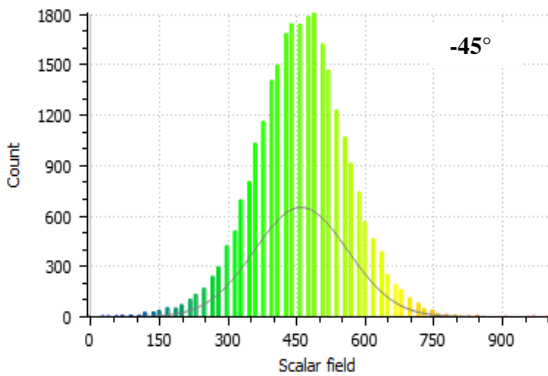
Gauss: mean = 720.247375 / std.dev. = 136.721603 [189 classes]



Gauss: mean = 633.163818 / std.dev. = 120.754936 [181 classes]



Gauss: mean = 459.599792 / std.dev. = 101.501869 [164 classes]



Note: The scalar field on the X-axis of all the graphs represents the intensity and it is a dimensionless value

Fig. 6: Intensity data distribution at various incidence angles

With reference to Fig. 6, two statistical parameters i.e. intensity mean and standard deviations were further investigated in exploratory data analysis of the intensity return at the various incidence angles. The data is normally distributed in all cases and as expected. In terms of the frequency, although the maximum count of 1800 was achievable at all incidence angles, the overall maximum mean intensity return was higher at normal angle of incidence where the point density is also high due to the nature of static TLS. Furthermore, as already pointed out in Fig. 5, the standard deviation grows with the intensity mean in Fig. 6.

4.2 Intensity and Incidence Angle (Before Correction)

The blocks were scanned at various incidence angles with the distance at each scanning station held fixed. Fig. 7 and 8 show the resultant relationship between uncorrected intensity for all the blocks and the scanning angle of incidence.

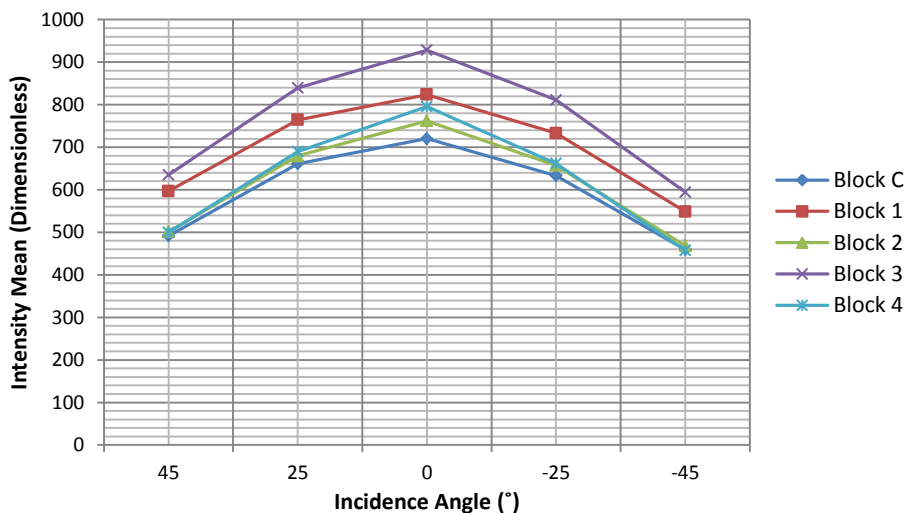


Fig. 7: Uncorrected intensity against incidence angle

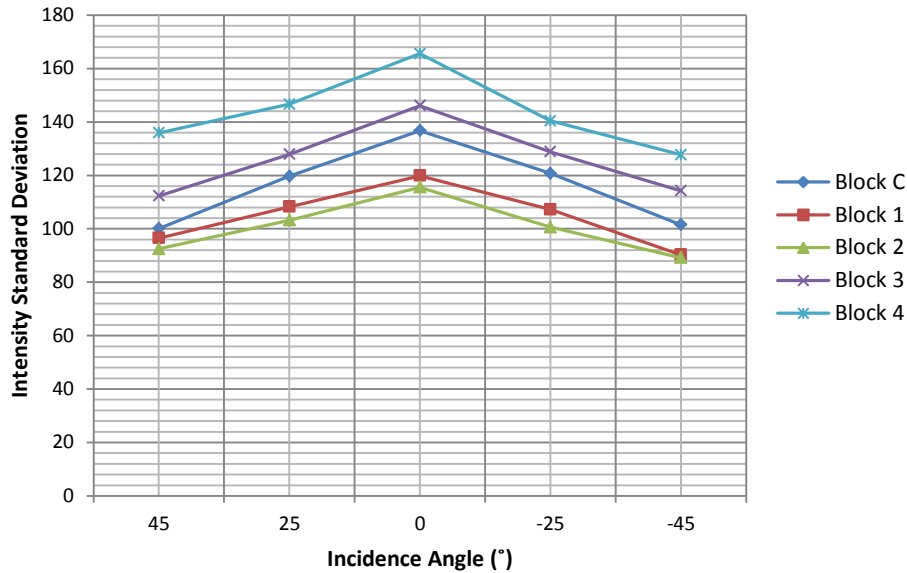


Fig. 8: Uncorrected intensity standard deviation against incidence angle

The incidence angle effect in both Fig. 7 and 8 is visible and all blocks show the trend where the intensity decreases as the incidence angle increases and this is true theoretically, based on the radar range equation. As reported in theory, it can be seen that the closer the laser beam incidence angle is to 0° the more the returned intensity. Generally, higher incidence angles lead to a reduction in the amount of returned intensity and this becomes more pronounced when incidence angles are greater than 20° (Krooks *et al.*, 2013) and for a Lambertian reflecting surface, the returned intensity has been predicted to decrease with the cosine of the incidence angle in accordance with Lambert's cosine law (Eq. (18)):

$$I_{raw} \propto P_r = K \cos \alpha \quad [18]$$

Although Eq. (18) is a simplified mathematical law and the light scattering behaviour of all natural surfaces is not Lambertian, the incidence angle dependence for many surfaces is approximated to follow the $\cos \alpha$ relation (Kaasalainen *et al.*, 2009b) as exemplified above.

4.3 Intensity and Distance (Before Correction)

The assessment of the distance effects on the intensity involved keeping fixed the various incidence angles and only varying the distances when scanning the concrete blocks. The relationships between the uncorrected intensity and the distance are as shown in Fig. 9.

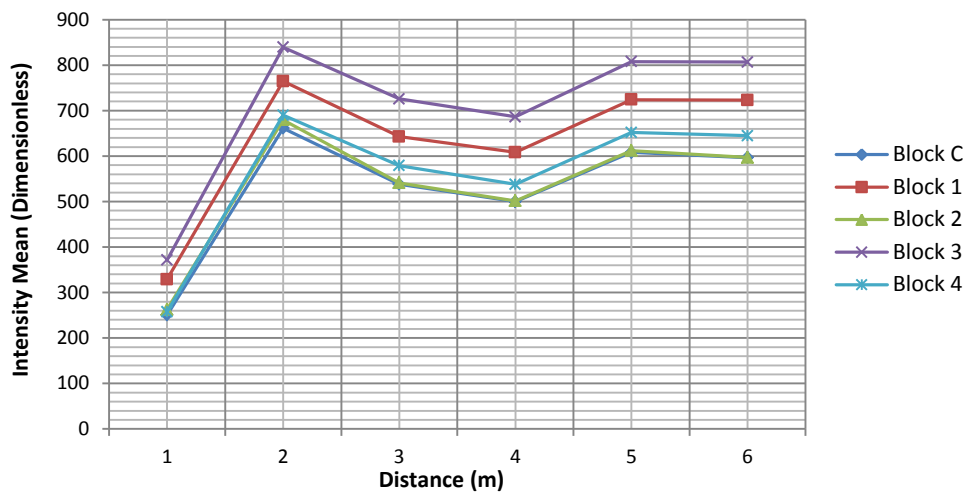


Fig. 9: Uncorrected intensity against distance

The distance effects on the intensity can be seen since in theory, the returned intensity is expected to decrease with an increase in distance. The plausible reason for the unexpected results was attributed to the instrumental effects at short scanning distances and such results have also been reported by other researchers (e.g. Kaasalainen *et al.*, 2011) although different scanners were used. Furthermore, in the same vein, Höfle (2014) states that past studies on TLS radiometric correction have clearly shown that the range dependence of TLS amplitude and intensity does not entirely follow the $1/R^2$ law of the radar equation as mostly valid for ALS, in particular at near distance of for instance less than 15 m. The reasons can be detector effects (e.g., brightness reducer, amplification, and gain control or receiver optics (defocusing and incomplete overlap of beam and receiver field of view). However, most manufacturers do not provide enough insight into developing a model-driven correction of these effects.

4.4 Intensity and Cosine Law Prediction vis-à-vis Incidence Angle

The theoretical contribution of the incidence angle to the deterioration of the returned intensity is plotted in Fig. 10 and it follows Eq. (18). The function $1/\cos(\alpha)$ was also applied and it gave the same result in Fig. 10 and according to Yan and Shaker (2014), this is why the cosine of the incidence angle is commonly taken to be indirectly proportional to the corrected intensity (or spectral reflectance) in the correction process.

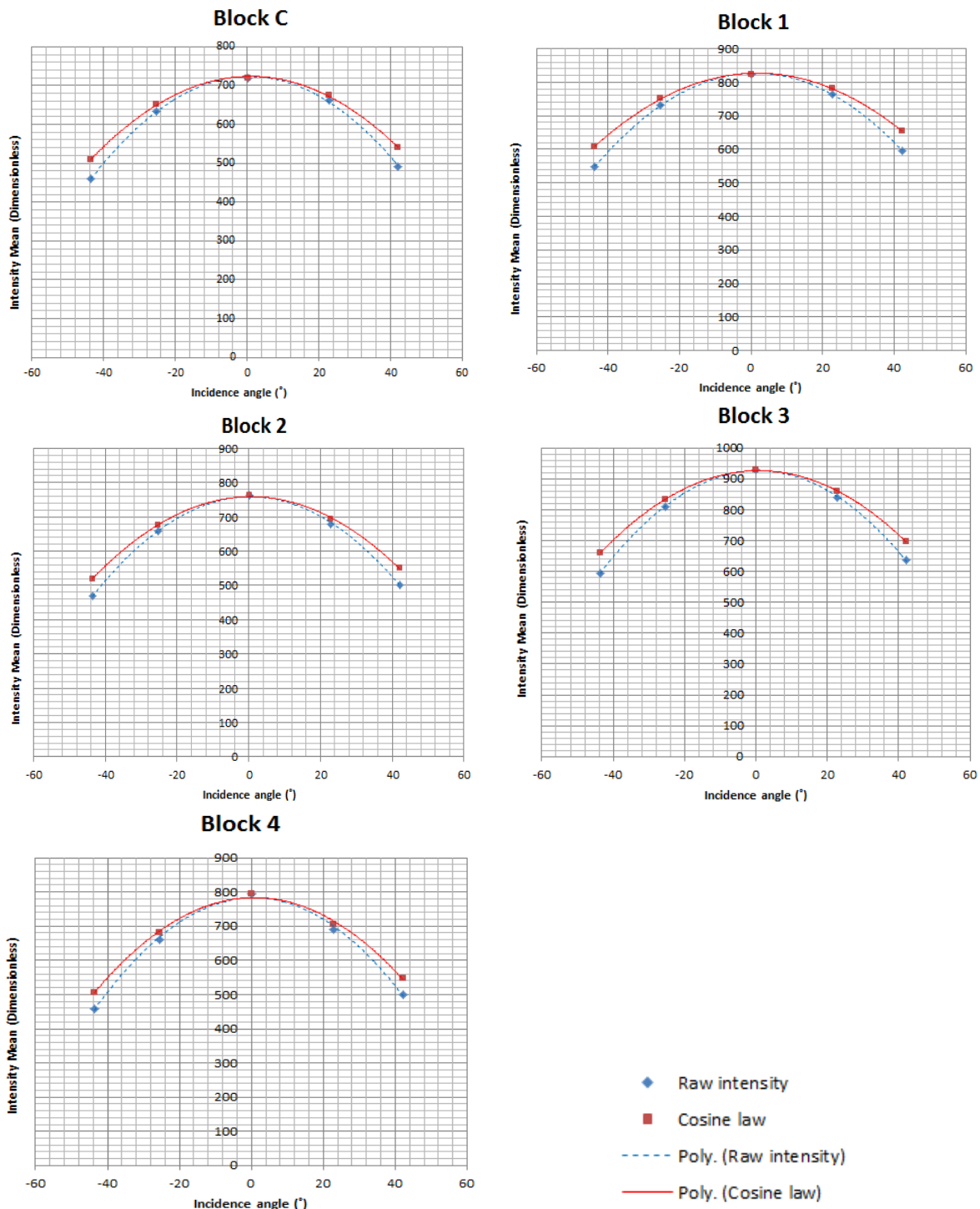


Fig. 10: Raw intensity and cosine law against incidence angle

The relationship between the intensity and the incidence angle as well as Lambert’s cosine law is shown in Fig. 10. A close correlation between the raw intensity and that with the cosine law is evident though a constant and an offset of the cosine of the incidence angle may have to be added for more accurate results as suggested in Kaasalainen *et al.* (2011). However, Lambert’s cosine law still provides a good approximation of the incidence angle effects, especially up to about 20° of incidence (Kaasalainen *et al.*, 2009b). Lambert’s cosine law can provide a satisfactory estimation of light absorption modelling for rough surfaces in both active and near-infrared spectral domains, thus, it is widely employed in existing intensity correction applications. However, Lambert’s cosine law is insufficient to correct the incidence angle effect for surfaces with increasing irregularity because these surfaces do not exactly follow the Lambertian scattering law. The incidence angle is related to target scattering properties, surface structure and scanning geometry. The interpretation of the incidence angle effect in terms of target surface properties is a complicated task (Tan and Cheng, 2016). However, Lambert’s cosine law has been successfully applied in some studies to correct the intensity for incidence angle effects. For instance, in Pfeifer *et al.* (2007) an experiment is reported with an Optech ILRIS3D laser scanner, where one target with near Lambertian scattering characteristics scanned at a distance close to 7m was observed at different angles. The intensity was corrected using the cosine correction and a linear amplification model.

To visualize the effect of the cosine law on the intensity values in overall scale, the average difference between the raw and cosine predicted intensity data points was plotted as shown in Fig. 11(a) for Block C as an example. Fig. 11(b) shows the raw intensity of Block C and the error bars indicate the average standard deviation.

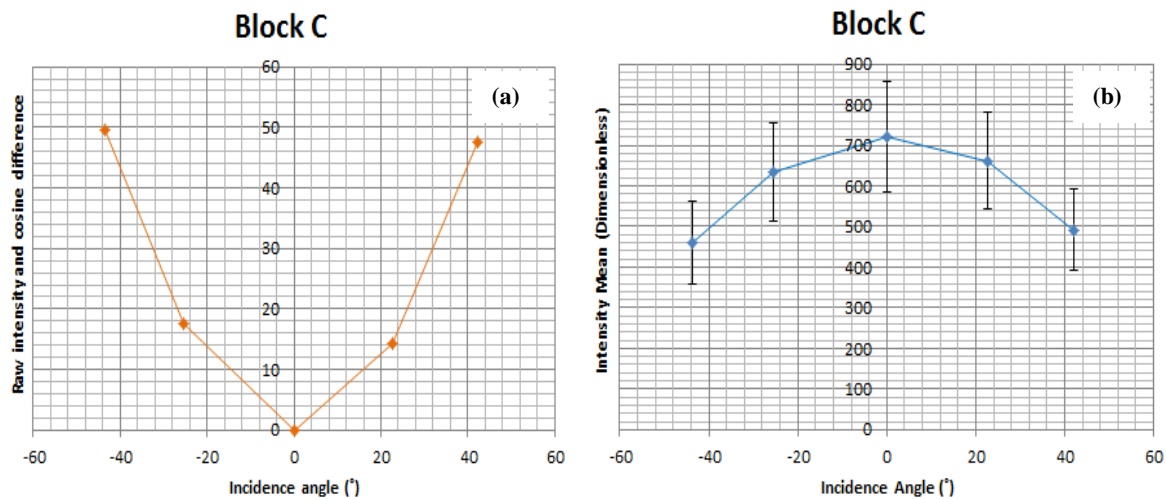


Fig. 11: Difference between raw intensity and cosine law against incidence angle

Compared to the error range of the intensity for Block C in Fig. 11(b), the difference between the raw intensity and that with the cosine law is still quite minimal, which in percentage terms ranges from 0% at normal incidence angle to about 11% at 45°. This means that the accuracy of the cosine

law is sufficient to predict the reflectance at this level of accuracy but may have limitations at higher angles of incidence as already pointed out above. However, the improved intensity correction method did not rely on the cosine law for incidence angle correction since it is insufficient to consider target surface characteristics, and more so its limitations beyond 20° of incidence angle.

4.5 Improved Intensity Correction Method

The procedural steps for the improved intensity correction method involve, first correcting intensity data for near-distance effects which are evident in Fig. 9 by applying the near-distance correction method presented above and after that the incidence angle and distance effects on the intensity can be solved separately since they do not mix.

According to Fang *et al.* (2015), in a study where the Z+F Imager 5006i laser scanner was used, the parameters in Eq. (9) have a physical basis and that the derived parameters in Table 2 were estimated in accordance with observed values such as the receiver's diameter and the detector's distance from the lens plane by iterative curve fitting using a nonlinear least squares method and robust Gauss-Newton algorithm. However, the values of the parameters differ for the various laser scanners and so each laser scanner needs to be studied.

Table 2: Values of Estimated Parameters

Parameters	$r_d(m)$	$d(m)$	$D(m)$	$s_d(m)$	$f(m)$
Lower	0.0	-1.0	0.03	0.01	0.05
Upper	0.005	0.2	0.6	0.9	0.5
Initials	1e-3	-0.18	0.05	0.18	0.15
Optimized	2.5e-3	-0.7538	0.05035	0.1608	0.1704

Although the estimated parameters in Table 2 were obtained using the Z+F Imager 5006i laser scanner, the parameters were tested for the HDS7000 laser scanner with success since the two instruments are coaxial and basically identical in terms of their physical characteristics as designed by the manufacturer. Fig. 12 below shows the results after applying the near-distance correction and it can be seen that the correction is valid for distances from 2m and greater since all the other scanning distances investigated follow the theoretical range squared inverse law in relation to the returned intensity and the measured distances. As already alluded to above, instrumental effects such as near-distance reducers (which are meant to avoid over-exposure of the sensor) are known to have an influence on the returned intensity and this actually makes the laser range equation to be inapplicable at all distances as a physical model for intensity correction.

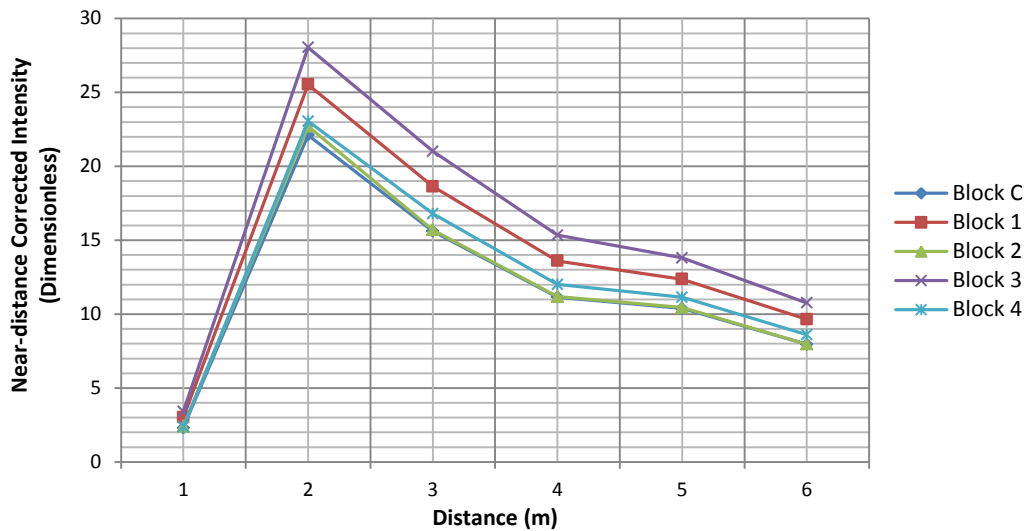


Fig. 12: Near-distance corrected intensity against distance

4.5.1 Intensity and Distance (After Correction)

Fig. 13 below shows the results of the relationship of intensity against distance after applying correction on the intensity data. With the exception of 1m, the correction is valid from 2m and all the other distances that the concrete was scanned from.

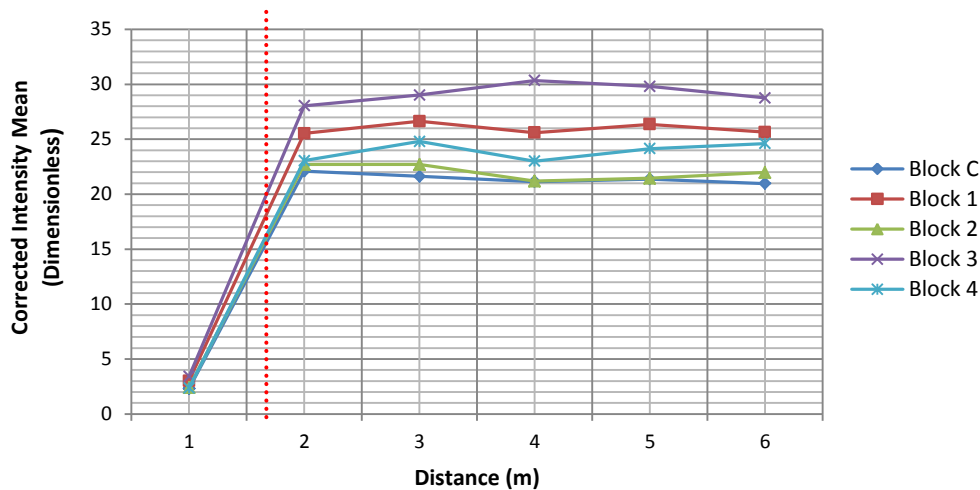


Fig. 13: Corrected intensity against Distance

4.5.2 Intensity and Incidence Angle (After Correction)

The relationship of the corrected intensity against incidence angle is as shown in Fig. 14. It can be observed that for all the angles of incidence that were investigated, the intensity correction method

is valid. The incidence angle effect on the intensity decreased as the graphs for all the blocks tend to straighten cross the whole range of the incidence angles.

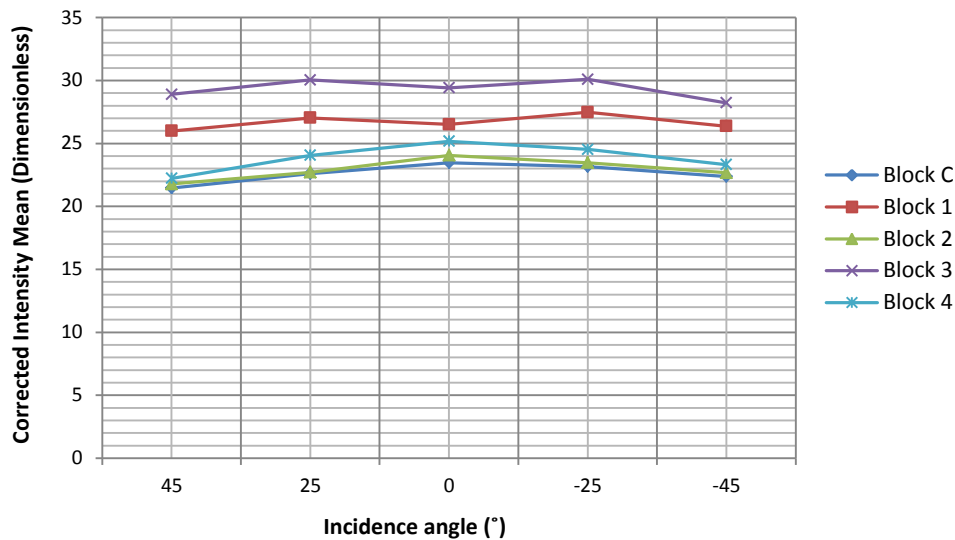


Fig. 14: Corrected intensity against incidence angle

Although the incidence angle effects appear to have significantly reduced in Fig. 14, the dominance of the reflectance for each block on the incidence angle behaviour can be seen and this could be because the blocks were not completely the same.

5. DISCUSSION AND CONCLUSION

The effects of the distance and incidence angle on the intensity of concrete specimens have been analysed by looking at the relationship of each with the intensity and they were found to be independent as also reported by some past researchers and this makes it possible to correct both by using different models that are independent of the measurement. Results of the uncorrected intensity and distance relationship have shown that intensity measurements from the HDS7000 scanner at near distances have instrumental effects and several other researchers as mentioned in the reviewed material have reported a similar finding even though different types scanners were used. The distance and incidence angle effects for the HDS7000 concrete intensity data were corrected using the improved method and this method has shown the potential to correct the intensity at scanning distances from 2m and greater. The correction of intensity for near distance effects is important for studies that require measurements to be taken at shorter baselines. The raw intensity in relation to that with the cosine law prediction did show a close relationship indicating that the cosine law provides a good approximation of the incidence angle effects and the more reason it is used in intensity correction schemes. However, Reshetyuk (2006) observed that the intensity return decreased with an increase in angle of incidence through experiments carried out using the

HDS3000 scanner although the scanned target (a wall) was not Lambertian. It has been reported in some studies that even when the raw intensity may appear to follow the cosine law prediction, there is no guarantee that the Lambert's cosine law would correct the intensity data for incidence angle effects as for instance pointed out in Tan and Cheng (2016) where a FARO Focus^{3D} 120 scanner was used and a different intensity correction method was actually applied. Furthermore, they have stated that the incidence angle is related to target scattering properties, surface structure and scanning geometry and that the interpretation of the incidence angle effect in terms of target surface properties is a complicated task. Surface roughness of the scanned target is also a factor that can influence the returned intensity and the concrete that was used in this study had roughness ranging from millimeters to a few centimeters. Although the magnitude of concrete roughness may seem to be small, it had an influence though minimal on the intensity correction. An improved intensity correction method such as the one presented could be potentially beneficial in several applications such as change detection, material classification and segmentation.

The following conclusions have been drawn from this study and in relation to the wider context of the subject in past research work:

1. An intensity correction model that considers near distance effects and also integrates the Oren-Nayar model so as to account for target roughness has been presented. The results achieved in the study are promising though more work still needs to be done as pointed out in the section for suggested areas of further research.
2. Several researchers have investigated the subject of TLS intensity correction as shown in the material that has been reviewed and it seems that a standard intensity correction method for all the different types of scanners does not exist yet. However, in Tan and Cheng (2015) it is argued that the proposed correction model can be applied to correct intensity data acquired with any scanner. This calls for more scanners to be tested.
3. The fact that different intensity correction methods have so far been proposed and some of which are complex, implies that the intensity fluctuations for any type of scanner may not be easily modelled. Furthermore, there is need to know what each scanner records, whether it's the intensity or the amplitude.
4. Instrumental effects on the returned intensity vary depending on the type of scanner and the manufacturer. However, for most scanners, the intensity-distance correction tend to be affected more by instrumental effects and these occur either for measurements taken at shorter baselines or those taken at longer baselines. This implies that the performance of each scanner has to be properly studied.

SUGGESTIONS OF FUTURE RESEARCH

1. The subject of TLS intensity correction is still an open area of investigation and this research is still on-going and future research will consider using the spectrometer and the VNIR hyperspectral camera (which operate at the wavelength of the TLS) for extracting spectral characteristics of the concrete specimens.
2. The concrete blocks that were used in this study were not significantly rough and so future

research work will test the method to correct intensity data of scanned objects with significant rough surfaces and with measurements taken at close range as was done in this study. Furthermore, correction for the incidence angle effects will need to be compared to that based on the linear combination of the Lambertian and Beckmann law.

3. Most TLS intensity correction methods that have been proposed in some past research work have often used targets of known reflectivity such as spectralons for calibration purposes to obtain the device constants or to determine the effects of near-distance reducers. There is need to test some of the correction methods with several natural targets.

ACKNOWLEDGEMENTS

The Authors express their gratitude to The University of Nottingham Ningbo China for the financial support and massive contribution in terms of the research facilities which made this study to be undertaken and many thanks to the FIG Foundation for co-funding the work through the scholarship which was awarded to the PhD student.

REFERENCES

- Anttila, K, Kasalainen, S, Krooks, A, Kaartinen, H, Kukko, A, Manninen, T, Lahtinen, P and Siljamo, N (2011) Radiometric Calibration of TLS Intensity: Application to Snow Cover Change Detection. *International Archives of the Photogrammetry, Remote Sensing and Spatial Information Sciences*, 38 (5/W12), 175-179.
- Balduzzi, M.A.F, Van der Zande, D, Stuckens, J, Verstraeten, W.W and Coppin, P. (2011) The properties of terrestrial laser system intensity for measuring leaf geometries: A case study with conference pear trees (*Pyrus Communis*). *Sensors*, 11, 1657-1681.
- Blaskow, R and Schneider, D (2014) Analysis and Correction of the Dependency between Laser Scanner Intensity Values and Range. *The International Archives of the Photogrammetry, Remote Sensing and Spatial Information Sciences*, Volume XL-5, 2014. ISPRS Technical Commission V Symposium, 23 – 25 June 2014, Riva del Garda, Italy.
- Carrea, D., Abellan, A., Humair, F., Matasci, B., Derron, M. and Jaboyedoff, M. (2016) Correction of terrestrial LiDAR intensity channel using Oren–Nayar reflectance model: An application to lithological differentiation. *ISPRS Journal of Photogrammetry and Remote Sensing*, 113, 17-29.
- Fang, W, Huang, X, Zhang, F and Li, D (2015) Intensity Correction of Terrestrial Laser Scanning Data by Estimating Laser Transmission Function. *IEEE Transactions on Geoscience and Remote Sensing*, 53, (2) 942-951
- Franceschi, M., Teza, G., Preto, N., Pesci, A., Galgrao, A. and Girardi, S. (2009) Discrimination between marls and limestones using intensity data from terrestrial laser scanner. *ISPRS Journal of Photogrammetry and Remote Sensing*, 64, 522–528.
- Habib, A, Kersting, A, Shaker, A and Yan, W.Y. (2011) Geometric Calibration and Radiometric Correction of Lidar data and their Impact on the Quality of Derived Products, *Sensors*, 11 (9) 9069-9097.

- Höfle, B. (2014) Radiometric Correction of Terrestrial LiDAR Point Cloud Data for Individual Maize Plant Detection. *IEEE Geoscience and Remote Sensing Letters*, 11(1) 94-98.
- Höfle B and Pfeifer N. (2007) Correction of laser scanning intensity data: Data and model-driven approaches. *ISPRS Journal of Photogrammetry and Remote Sensing*. 62 (6) 415-433.
- Jelalian, A. V (1992) *Laser Radar Systems*, Artec House, Norwood, MA USA.
- Kaasalainen, S, Jaakkola, A, Kaasalainen, M, Krooks, A and Kukko, A (2011) Analysis of Incidence Angle and Distance Effects on Terrestrial Laser Scanner Intensity: Search for Correction Methods. *Remote Sensing*, 3, 2207-2221.
- Kaasalainen, S, Krooks, A, Kukko, A and Kaartinen, H. (2009a) Radiometric calibration of terrestrial laser scanners with external reference targets. *Remote Sensing*, 1 (3) 144-158.
- Kaasalainen, S, Vain, A, Krooks, A and Kukko, A (2009b) Topographic and distance effects in laser scanner intensity correction, in: *Laser scanning 2009, IAPRS*, pp. 219–223.
- Kaasalainen S, Kukko A, Lindroos T, Litkey P, Kaartinen H., Hyyppä J, Ahokas E. (2008) Brightness Measurements and Calibration with Airborne and Terrestrial Laser Scanners. *IEEE Transactions on Geoscience and Remote Sensing*. 46 (2) 528–534.
- Krooks, A, Kaasalainen S, Hakala T, and Nevalainen, O (2013) correction of intensity incidence angle effect in terrestrial laser scanning *ISPRS annals of the photogrammetry, remote sensing and spatial information sciences*, volume II-5/w2, *ISPRS workshop laser scanning 2013*, 11-13 November 2013, Antalya, Turkey.
- Larsson, H., Hallberg, T., Elmqvist, M., Gustafsson, F. (2010) Background and target analysis from a Ladar perspective - Reflectance and penetration properties. FOI-R-- 3014 –SE ISSN 1650-1942.
- Leica Geosystems (2012) *HDS7000 User Manual* (on-line) <http://hds.leica-geosystems.com>, accessed on 14th July 2014.
- Oren, M. and Nayar, S. K. (1994). Seeing beyond Lambert's law. *Computer Vision — ECCV '94: Third European Conference on Computer Vision Stockholm, Sweden, May 2–6 1994 Proceedings, Volume II*. J.-O. Eklundh. Berlin, Heidelberg, Springer Berlin Heidelberg: 269-280.
- Oren, M. and Nayar, S. K. (1995) Generalization of the Lambertian model and implications for machine vision. *International Journal of Computer Vision*, 14(3), 227-251.
- Penasa, L, Franceschi, M, Preto, N, Teza, G and Polito, V (2014) Integration of intensity textures and local geometry descriptors from Terrestrial Laser Scanning to map chert in outcrops. *ISPRS Journal of Photogrammetry and Remote Sensing*, 93, 88-97.
- Pfeifer, N, Dorninger, P, Haring, A. and Fan, H (2007) Investigating terrestrial laser scanning intensity data: quality and functional relations. *Proceedings of VIII Conference on Optical 3D Measurement Techniques*, ETH Zurich, Switzerland (2007), pp. 328–337
- Reshetyuk, (2006) *Investigation and Calibration of Pulsed Time-of-Flight Terrestrial Laser Scanners*. Ph.D. thesis, Royal Institute of Technology (KTH), Division of Geodesy, Stockholm, Sweden.
- Shan, J and Toth, C.K. (2009) *Topographic Laser Ranging and Scanning: Principles and Processing*, CRC Press.
- Soudarissanane, S., Lindenbergh, R., Menenti, M. and Teunissen, P. (2009) *Incidence Angle*

- Influence on the Quality of Terrestrial Laser Scanning Points. *International Archives of the Photogrammetry, Remote Sensing and Spatial Information Sciences*, 38 (3/W8), 183-188.
- Soudarissanane, S, Lindenbergh, R, Menenti, M. and Teunissen P. (2011) Scanning Geometry: Influencing Factor on the Quality of Terrestrial Laser Scanning Points. *ISPRS Journal of Photogrammetry and Remote Sensing*, 66 (4) 389-399.
- Tan, K. and Cheng, X. (2015) Intensity data correction based on incidence angle and distance for terrestrial laser scanner. *Journal of Applied Remote Sensing*, 9, 094094:1–094094:22.
- Tan, K. and Cheng, X. (2016) Correction of Incidence Angle and Distance Effects on TLS Intensity Data Based on Reference Targets. *Remote Sensing*, 8 (3) 251.
- Tan, K., Cheng, X., Ding, X. and Zhang, Q. (2016) Intensity data correction for the distance effect in terrestrial laser scanners. *IEEE Journal of Selected Topics in Applied Earth Observations and Remote Sensing*, 9, 304–312
- Vain, A and Kaasalainen, S. (2011) Correcting Airborne Laser Scanning Intensity Data, *Laser Scanning, Theory and Applications*, Prof. Chau-Chang Wang (Ed.), ISBN: 978-953-307-205-0, InTech, DOI: 10.5772/15026. Available from: <http://www.intechopen.com/books/laser-scanning-theory-and-applications/correcting-airborne-laser-scanning-intensity-data>
- Yan, W.Y and Shaker, A. (2014) Radiometric Correction and Normalization of Airborne LiDAR Intensity Data for Improving Land-Cover Classification, *IEEE Transactions on Geoscience and Remote Sensing*, 52 (12) 7658-7673.
- Zhu, X., T. Wang, T., Darvishzadeh, R., Skidmore, A. K. and Niemann, K. (2015) 3D leaf water content mapping using terrestrial laser scanner backscatter intensity with radiometric correction. *ISPRS Journal of Photogrammetry and Remote Sensing*, 110, 14-23.

BIOGRAPHICAL NOTES

Wallace Mukupa is a post graduate research student in the Department of Civil Engineering at The University of Nottingham, Ningbo, China. He is currently pursuing a PhD in Engineering Surveying of civil structures.

Gethin W. Roberts is a Reader in Geospatial Engineering at The University of Nottingham, United Kingdom. He is the UN Delegate for the FIG through the Chartered Institution of Civil Engineering Surveyors. He is a past chairman of FIG Commission 6.

Craig M. Hancock is an Assistant Professor in Geospatial Engineering at The University of Nottingham, Ningbo, China. He is also involved with the International Federation of Surveyors (FIG) and has been a Vice Chair for communications on Commission 6 (Engineering Surveys) from 2010 – 2013.

Khalil Al-Manasir is an Assistant Professor in Geospatial Engineering at Middle East University, Amman, Jordan. He has worked at The University of Nottingham, Ningbo, China before as Assistant Professor.

CONTACT

Wallace Mukupa
The University of Nottingham, Ningbo, China.
Faculty of Science and Engineering
Department of Civil Engineering
199 Taikang East Road
Ningbo 315100
CHINA
Email: wallace.mukupa@nottingham.edu.cn